RELAXATION CHARACTERISTICS OF ALFALFA STEMS

Thesis for the Degree of PH D
MICHIGAN STATE UNIVERSITY
Glenn E. Hall
1966



This is to certify that the

thesis entitled

RELAXATION CHARACTERISTICS OF ALFALFA STEMS

presented by

Glenn E. Hall

has been accepted towards fulfillment of the requirements for

Ph.D. degree in Agricultural Engineering

al w. Juli Major professor

Date 2/24/67

0-169



RELAXATION CHARACTERISTICS OF ALFALFA STEMS

By

Glenn E. Hall

AN ABSTRACT

Submitted to
Michigan State University
in partial fulfillment of the requirements
for the degree of

DOCTOR OF PHILOSOPHY

Department of Agricultural Engineering

ABSTRACT

RELAXATION CHARACTERISTICS OF ALFALFA STEMS

by Glenn E. Hall

The theory of viscoelastic relaxation as applied to eight percent moisture content alfalfa stems is presented. The variations of the cross-sectional areas along the stems were determined and analyzed. An end view of stem sections taken throughout one millimeter intervals was photographed and scanned with a Flying-Spot Particle Analyzer to determine the area. Various methods for designating the cross-sectional area were used and compared.

Each stem section was submitted to a relaxation test with the stress applied in a longitudinal direction. The data obtained are represented by the equation

loge stress = A + B loge time,

where A is the ordinate intercept and B is the slope of the curve. The slopes of the relaxation curves and the cross-sectional area measurements were analysed by the spectral density method to determine the dimensional and relaxation characteristics along the alfalfa stems.

The slope of the relaxation curve for the stem sections was very highly correlated with its neighboring sections up to a distance of 100 mm, which was the maximum distance included in the analysis. This indicates that the stem section selected for a relaxation test is not

critical. The area analysis showed that it is necessary to determine the area at or within 0.75 millimeters of the point of loading if satisfactory results are to be expected since there is considerable area fluctuation along the alfalfa stem.

Approved Calw. See

Major Professor and Department

RELAXATION CHARACTERISTICS OF ALFALFA STEMS

By (~)

A THESIS

Submitted to

Michigan State University
in partial fulfullment of the requirements
for the degree of

DOCTOR OF PHILOSOPHY

Department of Agricultural Engineering

1966

VITA

Date of Birth: 21 April 1931

Military Service: U. S. Army, Counter Intelligence Corps,

March 1954 to March 1956

Education: Scipio-Republic High School, Republic, Chio,

Graduated May 1949

Michigan State University, B.S., Mechanical

Engineering, June 1959

Michigan State University, M.S., Agricultural

Engineering, June 1960

M.S. Thesis: Conduction Drying of Shelled Corn

Employment: Farming to March 1954

Research Assistant, Michigan State University

June 1959 to June 1960

Instructor, Chio Agricultural Research and

Development Center, June 1960 to July 1965

Research Assistant, Michigan State University,

September 1963 to February 1965

Assistant Professor, Chio Agricultural Research

and Development Center, July 1965 to present

Ph.D. Oral Examination: 2 December 1966

ACKNOWLEDGMENTS

I wish to express my appreciation to the following persons for their assistance during my graduate program:

Dr. Carl W. Hall, my Major Professor, whose guidance and encouragement throughout my graduate program were immensely invaluable and enjoyable;

Dr. Ross D. Brazee, whose counsel, guidance, and encouragement during the theoretical and experimental portions of the investigation were greatly appreciated;

Dr. Fred H. Buelow, Dr. Merle L. Esmay, Dr. Carter M. Harrison, and Dr. George E. Mase, members of my graduate guidance committee, for their counsel during my graduate program;

Dr. Robert E. Stewart and Dr. William H. Johnson for encouragement and assistance toward completion of the graduate program:

Mr. Roy Jordan and Mr. Norman Hostetler for their assistance during the experimental portions of this investigation;

Mr. Glenn Shiffer, Mr. Jim Cawood, and Mr. Harold Brockbank for their assistance during research performed while undertaking courses at Michigan State University;

Mrs. Doris Baum, whose typing assistance was certainly appreciated;

Rose, my wife, for her constant encouragement;

Christine and Melissa, my daughters, who will someday realize the implications of a graduate program;

And all others who contributed to my graduate program.

I also wish to express my appreciation for assistance by:

Ohio Agricultural Research and Development Center for financial assistance during my leave;

United States Department of Agriculture for the use of equipment during the experimental phases of this investigation.

And Massey-Ferguson Ltd. for partial financial assistance while in attendance at Michigan State University.

IIST OF CONTENTS

Section	<u>n</u>	Page
I.	INTRODUCTION	1
	A. Historical Background	1
	B. Experiments	2
	C. Alfalfa Stem Photomicrographs	3
II.	VISCOEIASTIC RELAXATION THEORY	7
III.	RELAXATION TIME SPECTRUM	11
IV.	STRESS RESPONSE IN A RANDOM VISCOELASTIC MEDIUM .	15
v.	EXPERIMENTAL INVESTIGATION	21
	A. Area Measurement	23
	B. Relaxation Tests	31
VI.	RESULTS AND DISCUSSION	34
	A. Comparison of Area Measurement Methods	34
	B. Methods of Analysis	39
	C. Area Spectral Density and Correlation	110
	D. Relaxation Spectral Density and Correlation .	41
VII.	CONCLUSIONS	46
	A PPENDIY	47
	RECOMMENDATIONS FOR FUTURE STUDY	48
	REFERENCES	49
	INDEX	51

LIST OF TABLES

Table		Page
1.	Internodal distances of two alfalfa stems used for	
	area and relaxation characteristic fluctuations	. 21
2.	Internodal distances of alfalfa stems used for area	9
	determination comparisons	, 22
3.	Comparison of cross-sectional area measurements	. 35
4.	Spectral analysis program for IBM 1620 computer	. 37

LIST OF FIGURES

Figure		Page
1.	Photomicrograph at 77X magnification of quarter cross-section of alfalfa stem	4
2.	Photomicrograph at 350X magnification of alfalfa stem eipdermis	
3.	Photomicrograph at 1,37X magnification of longitudinal Section of alfalfa stem	5
4.	Examples of film negatives of stem cross-sectional views as used in Flying-Spot Particle Analyzer for area measurement	25
5.	Flying-Spot Particle Analyzer used to determine stem cross-sectional areas	26
6 a.	Block diagram of Flying-Spot Particle Analyzer film scenner	27
6 0.	Block diagram of Flying-Spot Particle Analyzer logic circuits	28
7.	Cut-off saw used to section alfalfa stems	30
8.	Device for conducting relaxation experiments of alfalfa stem section	30
9.	Two stress relaxation curves obtained during the investigation	33
10.	Spectral density and correlation for alfalfa stem cross-sectional areas	42
11.	Snectral density and correlation of slopes of alfalfa stem relaxation curves	կկ

I. INTRODUCTION

The more information there is concerning the properties of a product the more rational becomes the design procedure for new machines and processes to utilize the product. An economical approach for new machinery design in the agricultural area would be to determine the requirements of the product before designing the machine. Prior knowledge of a product's properties would save considerable time and expense in machine development research. Product properties will assist in machine design, but will not eliminate all empirical approaches since we cannot completely describe every situation.

Prior to conducting extensive tests concerning the physical properties of forages we should have information concerning product variations within a single unit as well as between similar products.

The aim of this investigation was to determine the variation of the cross-sectional area and relaxation characteristics of alfalfa stems as a function of position along the stem. This information will be useful to researchers investigating the properties of alfalfa by indicating fluctuations which are normally present and indicating the care which must be exercised if reliable results are to be obtained.

A. Historical Background

Alfalfa is an herbaceous perennial legume that may live 15 to 20 years or more unless destroyed by insects or disease. The most commonly cultivated species is Medicago sativa, which includes the purple-flowered Vernal alfalfa variety.

The name alfalfa, which comes from the Arabic language, means best fodder. It is generally called lucerne in Europe and is believed to have originated in southwestern Asia. Alfalfa was first cultivated in Iran, then Arabia and the Mediterranean countries, and finally carried to the New World. The first recorded attempt to raise alfalfa in the United States was in Georgia in 1736. Its introduction into California from Chile in about 1850 started a rapid expansion in alfalfa acreage.

The alfalfa plant varies from two to three feet in height and has 20 or more erect stems that continue to grow from the crown branch as the older stems are harvested. Many short branches may grow from each stem and the oblong leaves, arranged alternately on the stem, are pinnately trifoliate. The root system consists of an almost straight taproot—sometimes growing to a depth of 25 to 30 feet—from which side branches extend short distances. The fruit of alfalfa is a spirally twisted pod containing the small seeds. Further information concerning alfalfa cultivation can be found in Martin and Leonard (1949) and Hayward (1938).

B. Experiments

There are two types of rheological experiment for obtaining viscoelastic properties; transient and dynamic. Included in the transient tests are relaxation, creep, and constant strain rate experiments. The dynamic tests include steady-state sinusoidal and non-sinusoidal, and impact experiments.

The alfalfs stem sections used in this investigation behaved as viscoelastic material, rather than viscoplastic, because the dimensional characteristics of the stem sections were the same before and after the

stress loading cycle. If plastic deformation did occur it was not possible to observe the dimensional changes after stress removal with the use of the microscope.

C. Alfalfa Stem Photomicrographs

A photomicrograph, at 77X magnification, of a quarter cross-section of an alfalfa stem is shown in Figure 1. The various parts of the stem are labeled on the photomicrograph.

As the stem metures an interfascicular cambium develops, and a cambical cylinder develops which produces a continuous zone of lignified xylem. Some of the smaller parenchymatous (thin-walled) cells on the inner face of the bundles may become lignified. The stem is also reinforced by a layer of collenchyma (thick-walled cells); the four corners of the stem are reinforced with several layers of collenchyma. The parenchymatous cells of the pith may disintegrate or become ruptured so that the mature stem becomes hollow. This is in evidence in the large open area of the pith shown in Figure 1.

Figure 2 is a photomicrograph of alfalfa stem epidermis at 350X magnification. The long dimension of the epidermal cells, (a), is parallel to the longitudinal direction of the stem. A stoma is shown at (b).

Figure 3 is a photomicrograph of a longitudinal section of alfalfa stem, at 437X magnification, showing the spiral tracheal tube, (a), and pitted tracheid, (b).

Additional details on the structure of alfalfa are given by Wilson and Loomis (1962), Wilson (1913), and Hayward (1938).

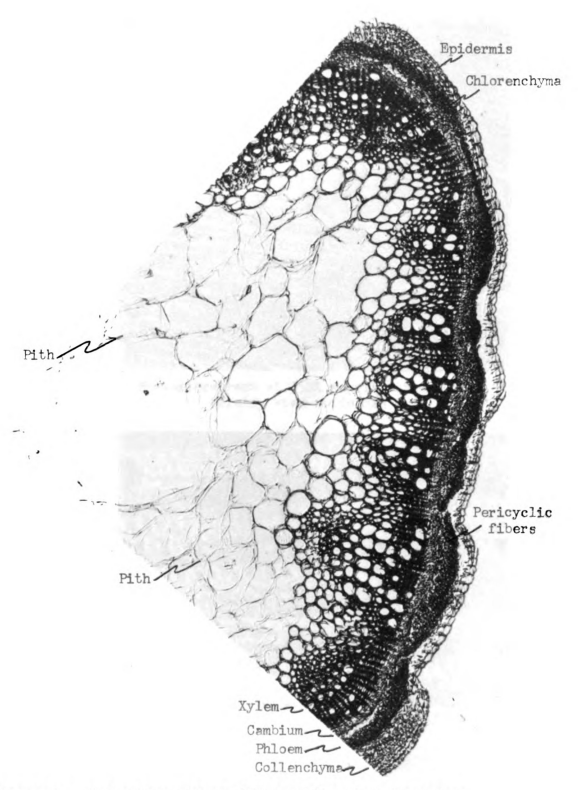
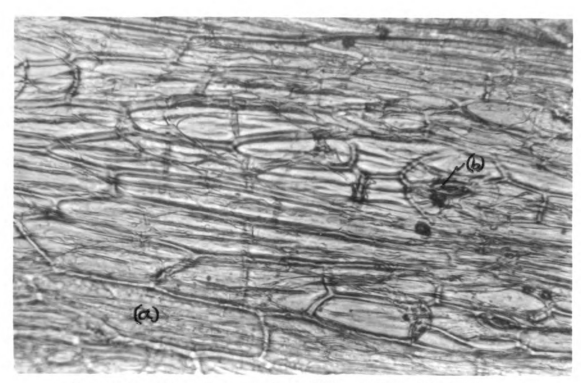


Figure 1. Photomicrograph at 77% magnification of owarter cross-section of alfalfa stem



Wigure 2. Photomicrograph at 350X magnification of alfalfa stem epidermis

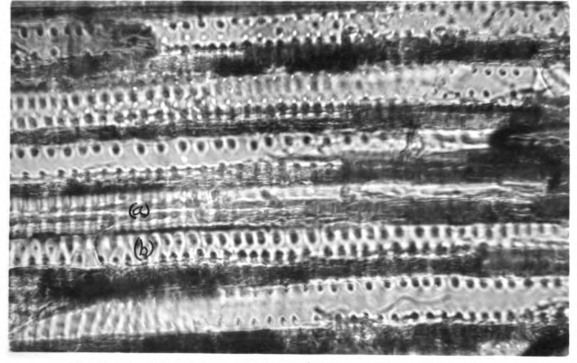


Figure 3. Photomicrograph at 137X magnification of longitudinal section of alfalfa stem

The cellular structure of the alfalfa stem consists of cross-linked and linear polymers which affect both the physical and chemical properties. From this it would be expected that alfalfa stems would behave in a manner similar to other viscoelastic polymers, and that mathematical techniques employed to define the behavior of other polymers could be applied to alfalfa stems.

II. VISCOELASTIC RELAXATION THEORY

Consider two neighboring points of a stress-free continuous medium and denote their separation by the infinitesimal vector

$$\underline{\delta} = \underline{i}\delta_{x} + j\delta_{y} \quad \underline{k}\delta_{z}.$$

When the medium is subjected to a stress, the two points will be displaced from their initial positions by \underline{r} and $\underline{r} + \Delta \underline{r}$, with point 1 displaced by \underline{r} and point 2 displaced by $\underline{r} + \Delta \underline{r}$. Since $\underline{\delta}$ and $\underline{\Delta}$ approach zero together, we expand $\underline{\Delta}\underline{r}$ to obtain, component-wise,

$$(\Delta c)_{x} = (\partial r_{x}/\partial x)\delta_{x} + (\partial r_{x}/\partial y)\delta_{y} + (\partial r_{x}/\partial z)\delta_{z}; \qquad (1)$$

$$(\Delta \underline{c})_{y} = (\partial r_{y}/\partial x)\delta_{x} + (\partial r_{y}/\partial y)\delta_{y} + (\partial r_{z}/\partial z)\delta_{z}; \qquad (2)$$

$$\Delta r)_{z} = (\partial r_{z}/\partial x)\delta_{x} + (\partial r_{z}/\partial y)\delta_{y} + (\partial r_{z}/\partial z)\delta_{z}, \qquad (3)$$

or, in vector form,

$$\Delta r = \delta \cdot \nabla r. \tag{4}$$

Following the approach of Fitts (1962), separate $\nabla_{\underline{\cdot}}$ into its symmetric and antisymmetric parts,

$$\nabla \underline{c} = \underline{e} + (\nabla \underline{c})_{\alpha}, \tag{5}$$

where $(\nabla \underline{r})_{\alpha}$ is antisymmetric, and the symmetric part $\underline{\epsilon}$ represents the strain on the medium. The antisymmetric part may be written

$$(\nabla \mathbf{r})_{\alpha} = -\frac{1}{2}(\underline{\nabla} \times \underline{\mathbf{r}}) \times \underline{\underline{\mathbf{U}}}, \tag{6}$$

where U is the unit dyadic (second-order tensor) defined as

$$\underline{\underline{U}} \times \underline{\mathbf{ii}} + \underline{\mathbf{jj}} + \underline{\mathbf{kk}}. \tag{7}$$

Since

$$\overline{\Delta} \cdot (\Delta \times L) = 0$$
 (8)

for any vector, the dyadic $(\nabla \underline{r})_{\alpha}$ is divergenceless and represents a pure rotation of the medium. Hence, it does not contribute to the strain and will hereafter be omitted. Next assume that the medium is <u>visco-elastic</u>, with stress and strain both functions of time. The stress and strain are related by the equation

$$\underline{\sigma}(t) = \underline{\mathfrak{U}} : \underline{\mathfrak{g}}(t) \tag{9}$$

where $\underline{\underline{u}}$ is a fourth-order tensor which transforms $\underline{\underline{c}}$ under the indicated operation into a new (stress) dyadic, $\underline{\underline{\sigma}}$.

If the Y6 component of the $\underline{\varepsilon}$ strain tensor experiences a unit step change at time t=0, then

$$\epsilon_{\gamma\delta} = 0$$
 for t<0,
 $\epsilon_{\gamma\delta} = 1$ for t>0. (10)

The response of the $\alpha\beta$ stress component to the unit step change in the $\gamma\delta$ strain component is denoted by $K_{\alpha\beta,\gamma\delta}(t)$, and this response, under the relaxation test of viscoelasticity, is a time function which is zero for t<0. Owing to the symmetry of $\underline{\epsilon}$, a change in $\epsilon_{\gamma\delta}$ is accompanied by an equal change in $\epsilon_{\delta\gamma}$ If $K_{\alpha\beta,\gamma\delta}$ is defined as one-half the sum of the responses $\epsilon_{\gamma\delta}$ and $\epsilon_{\delta\gamma}$, then $K_{\alpha\beta,\gamma\delta}$ is symmetric in γ and δ . Also, it must be symmetric in α and β since $K_{\alpha\beta,\gamma\delta}$ gives the $\alpha\beta$ stress component, which is known to be symmetric. As a consequence of these symmetries for σ and ϵ tensors.

$$K_{\alpha\beta,\gamma\delta}(t) = K_{\beta\alpha,\gamma\delta}(t) = K_{\alpha\beta,\delta\gamma}(t) = K_{\beta\alpha,\delta\gamma}(t).$$
 (11)

These quantities are the components of a fourth-order tensor $\underline{K}(t)$, as in Eq. (9), which in general would have 81 components in three-dimensional space but, due to the symmetries expressed in Eq. (11), has instead only 36 independent components.

Assuming the unit-strain response to be invariant under translation of the time origin, $\underline{K}(t-s)$ may be regarded as the response to a unit step in \underline{s} occurring at time s. When the temperature and other quantities which might affect the form of $\underline{K}(t)$ are constant or change slowly as compared with stress-strain changes in the medium, then this assumption will be valid. Upon assuming that the stresses may be compounded in a linear manner, the change $d\sigma_{\alpha\beta}(t)$ in the $\alpha\beta$ component of the stress tensor $\underline{g}(t)$ due to unit steps $d\varepsilon_{\gamma\delta}$ at time s in the $\gamma\delta$ component of the strain $\underline{s}(s)$ may be written as

$$d\sigma_{\alpha\beta}(t) = \sum_{\gamma} \sum_{\delta} K_{\alpha\beta,\gamma\delta}(t-s) d\epsilon_{\gamma\delta}(s). \qquad (12)$$

To find the stress on the medium at time t integrate Eq. (12) to obtain

$$\sigma_{\alpha\beta}(t) = \int_{-0}^{t} d\sigma_{\alpha\beta}(t) = \int_{-0}^{t} \sum_{\mathbf{Y}} \sum_{\delta} K_{\alpha\beta,\mathbf{Y}\delta}(t-s) d\mathbf{e}_{\mathbf{Y}\delta}(s)$$
 (13)

In the dyadic notation, Eq. (13) may be expressed as

$$\underline{\underline{\sigma}}(t) = \int_{-0}^{t} K(t-s) : d\underline{\underline{s}}(s).$$
 (14)

If the strain g undergoes a finite step at time s=0 and then has only continuous changes, Eq. (14) becomes

$$\underline{\underline{\sigma}}(t) = \underline{\underline{K}}(t) : \underline{\underline{\epsilon}}(0) + \int_{+0}^{t} \underline{\underline{K}}(t-s) : \dot{\underline{\epsilon}}(s) ds, \qquad (15)$$

where $\underline{\varepsilon}(0)$ is the finite change in strain at time s=0 and the lower limit of integration, +0, indicates that the finite change in $\underline{\varepsilon}$ at s=0 is excepted from the integration. The components of $\underline{\dot{\varepsilon}}$ are defined by

$$\epsilon_{\alpha\beta}(s) = d\epsilon_{\alpha\beta}(s)/ds.$$
 (16)

Recalling that $\underline{\underline{e}}$ is the symmetrical part ∇r , Eq.(16) can be written as

$$\dot{\epsilon}_{\alpha\beta}(s) = \frac{1}{2} d/ds (\partial r_{\beta}/\partial x_{\alpha} + \partial r_{\alpha}/\partial x_{\beta})$$

$$= \frac{1}{2} \left[\partial/\partial x_{\alpha} (\dot{c} r_{\beta}/\partial c) + (\partial/\partial x_{\beta}) (\partial r_{\alpha}/\partial s) \right]$$

$$= \frac{1}{2} (\partial u_{\beta}/\partial x_{\alpha} + \partial u_{\alpha}/\partial x_{\beta}) , \qquad (17)$$

where u_{α} is the α component of \underline{u} , the center-of-mass velocity. Hence, $\underline{\dot{e}}$ is the symmetrical part of $\nabla \underline{u}$.

III. RELAXATION TIME SPECTRUM

This section embodies an extension of the relaxation stress response theory as discussed in Section II. As a first step pertinent theory as outlined by Ferry (1901) is reviewed.

Any experimentally observed stress relaxation curve which decreases monotonically can, in principle, be fitted with any desired degree of accuracy to a series of exponential terms of sufficient number, each with its own relaxation time. If the number of terms or elements in the defining model is increased without limit, the result is a continuous spectrum in which each infinitesimal contribution to righty FdT is associated with relaxation times lying between T and T+dT. According to Ferry (1961) a logarithmic time scale is more convenient and the continuous relaxation spectrum is defined as HdlnT with relaxation times whose logarithms lie between lnT and lnT + dlnT. For the continuous spectrums we have

$$K(t) = F_e + \int_{-\infty}^{\infty} He^{-t/\tau} d(\ln \tau),$$
 (18)

which may be taken as the mathematical definition of H without the need of mechanical models language. The constant K_e is added to allow for a discrete contribution with $\tau=\infty$. The value of K_e is zero for uncross-linked polymers. The function H is multiplied by the intensity function $e^{-t/T}$ which goes from zero $\tau=0$ to 1 as τ approaches infinity. This is approximated by a step function going from zero to one at $\tau=t$. Therefore

$$K(t) \simeq K_e + \int_{1}^{\infty} Hd(1n\tau), \qquad (19)$$

and

$$H(\tau) \simeq - dK(t)/d(\ln t) \Big|_{t=\tau}$$
 (20)

or

$$H(\tau=t) = -dK(t)/d(\ln t)$$
 (21)

In terms of stress, $\sigma(t) = \varepsilon K(t)$, where ε is constant strain during the relaxation experiment. Substituting into Eq. (21) we obtain

$$H(\tau = t) = -(1/\epsilon)d\sigma(t)/d(\ln t). \tag{22}$$

According to Ferry and Williams (1952), if $H(\tau)$ is of the form $H(\tau)=k_1^{-\alpha}$ with

$$\sigma(t) = \epsilon \int_{-\infty}^{\infty} He^{-t/\tau} d(\ln \tau),$$

then

$$\sigma(t) = \int_{-\infty}^{\infty} k\tau^{-\frac{\alpha}{2}} e^{-t/\tau} d(\ln \tau) = k\varepsilon \int_{-\infty}^{\infty} \tau^{-\frac{\alpha}{2}} e^{-t/\tau} d\tau/\tau$$
$$= k\varepsilon \int_{0}^{\infty} \tau^{-\frac{\alpha}{2}-1} e^{-t/\tau} d\tau.$$

Letting $x = t/\tau$ and $d\tau = -tdx/x^2$, then

$$\sigma(t) = k\varepsilon \int_{0}^{\infty} (t/x)^{-n-1} e^{-x} (tdx/x^{2})$$

$$= k\varepsilon t^{-n} \int_{0}^{\infty} x^{n-1} e^{-x} dx$$

$$\sigma(t) = k\varepsilon \Gamma(m) t^{-n}, \quad m > 0,$$
(23)

where I (m) is the gamma function.

Inserting Eq. (23) into Ec. (22) yields

$$H(\tau=t) = H(\tau) = k\Gamma(m + 1)\tau^{-n},$$

in error by a factor of $\Gamma(m+1)$. But the second approximation may be

written

$$H(\tau=t) = -[1/\Gamma(m+1)] (1/\epsilon) [d\sigma(t)/d(\ln t)].$$
 (24)

Letting

$$M(m) = [1/\Gamma(m + 1)]$$
 (25)

and

$$K_1(t) = (1/\epsilon)\sigma(t),$$
 (26)

and noting that

$$dK_1(t)/d(\ln t) = K_1(t) d[\ln K_1(t)]/d(\ln t)$$
 (27)

so that

$$H(\tau) = \{-M(m)K_1(t)[dln K_1(t)/d(ln t)]\}_{t=\tau}$$
 (28)

Based on these procedures by Ferry (1961) and Ferry and Williams (1952), it is hypothesized that the relationship existing between stress and time for the alfalfa stem sections can be expressed as

$$\ln \sigma(t) = m \ln t - m \ln t_0 + \ln c_0, \qquad (29)$$

which can be changed to the form

$$\ln \left[\sigma(t)/\sigma_0\right] = -m \ln \left(t/t_0\right) \tag{30}$$

and

$$-m = \ln \left[\sigma(t) / \sigma_0 \right] / \ln \left(t / t_0 \right). \tag{31}$$

From Eq. (29),

$$\sigma(t)/\sigma_0 = (t/t_0)^{-1}, \qquad (32)$$

letting ke $\sigma_0 t_0^n$,

$$\sigma(t) - ket^{-1}$$
 (33)

and

$$H(\tau=t) = -(1/\epsilon)d\sigma(t)/d(\ln t)$$

$$= \left[-(1/\epsilon)k\epsilon t dt^{-\alpha}/dt\right]_{t=\tau} = km\tau^{-\alpha}$$
(34)

$$\sigma(t) = \epsilon \int_{-\infty}^{\infty} H_3^{-t/T} d(\ln \tau) = \epsilon \int_{-\infty}^{\infty} km\tau^{-1} e^{-t/T} d(\ln \tau)$$

$$= k\epsilon m \int_{0}^{\infty} \tau^{-m-1} e^{-t/T} d\tau = k\epsilon mt^{-m} \int_{0}^{\infty} x^{m-1} e^{-x} dx$$

$$= k\epsilon m \Gamma(m) t^{-m} = k\epsilon \Gamma(m+1) t^{-m}$$
(35)

and, after attaching the factor $[1/\Gamma(m+1)]$ to $H(\tau)$ for a second approximation,

$$H(\tau=t) = -[1/\Gamma(m+1)] (1/\epsilon) d\sigma(t)/d(\ln t).$$
 (36)

If $\sigma_0 = t_0 = 1$, Eq.(29) reduces to

$$\sigma(t) = t^{a} \tag{37}$$

which is actually of the form

$$\sigma(x,t) = t^{\pi(x)}$$
 (38)

since the stress and slope are functions of position and time, and position, respectively.

IV. STRESS RESPONSE IN A RANDOM VISCOELASTIC MEDIUM

The stress response is now considered as an homogeneous random function of position in a viscoelastic medium whose microstructure consists of grains, cells, or fibers of random sizes, lengths, diameters, or strength properties. Such structures could be generated, e.g., by growth processes of various kinds, biological materials being typical. It is implied that the physical parameter fluctuations can be described by distributions or correlations in the statistical sense. The random function describing the fluctuating stress response may be linearly separated into a uniform mean component and fluctuating component. Interest will center on the fluctuating component.

Assume that raw data are available from a series of viscoelastic experiments with a particular random medium. Further, suppose that these data have leen investigated, removing trends and periodicities of interest, and it is now desired to study the residual aperiodic fluctuations. A particular point to be investigated here is whether the random data are statistically homogeneous throughout the medium. This could be done in a preliminary way by observing whether statistical parameters or distributions persistently change in magnitude or form in various regions of the medium.

It seems appropriate to sketch this theory by starting with simple alterations of Eqs. (14) and (15), viz.,

$$\underline{\underline{\sigma}}(x,t) = \int_{0}^{t} \underline{\underline{K}}(\underline{x}, t-s) : \underline{\underline{\dot{s}}}(s) ds, \qquad (39)$$

or

$$\underline{\underline{\sigma}}(x,t) = \underline{\underline{K}}(\underline{x},t) : \underline{\underline{\varepsilon}}(0) + \int_{+C}^{t} \underline{\underline{K}}(x, t-s) : \underline{\underline{\dot{\varepsilon}}}(s) ds \qquad (40)$$

where now spatial dependence of the stress response prevails. The eighthorder correlation tensor is written

$$\underline{\underline{R}}(\underline{x}_1, \underline{x}_2) = \langle \underline{\underline{K}}(\underline{x}_1, t)\underline{\underline{K}}(\underline{x}_2, t) \rangle. \tag{41}$$

The fluctuations in viscoelastic properties, mainly relaxation characteristics, are important random fluctuations of position. These variations are partially described by a distribution function $P[\underline{K}(\underline{x},t)]$. The distribution function could, ideally, be estimated on the basis of experimental data. Knowing the distribution function, moments could be calculated,

$$= \int_{-\infty}^{\infty} [\underline{\underline{K}}(\underline{x},t)\underline{\underline{K}}(x,t) \dots \underline{\underline{K}}(\underline{x},t)]_{\text{order } n} d\underline{\underline{K}}(\underline{x},t)]. \quad (42)$$

Work by Beran (1965), using a similar approach for heterogeneous materials, was discovered after this portion of the theoretical background had been developed. Ideally, information would be available on the distribution of all components of $\underline{K}(\underline{x},t)$ which would yield the form of $\underline{F}(\underline{K}(\underline{x},t))$. But in physical problems it will be necessary to be content with considerably less. A complete description of the system could be given if the ideal situation existed. Instead approximate descriptions are available on limited information. It may be more profitable to make less detailed descriptions of more systems. The statistical-mathematical model based on less detail may be the most useful one available from the infinite number of models available.

Wiener (1956) has discussed modeling of physical systems on the basis of imprecise, but extensive information. An important point which he discusses is that highly precise measurements in some cases are not the best technique. The more extensive, less precise measurements may yield more real information and understanding of the actual system.

Blackman and Tukey (1958) also discuss the trouble that may be encountered by the investigator who attempts to apply overprecise measurements to problems in physical research.

Now, letting \(\lambda \) represent a particular time t, Eq. (38) becomes

$$\sigma(x,\lambda) = \lambda^{n(x)} \tag{43}$$

and, for different locations on the stem, x_1 and x_2

$$σ(x1, λ) = λ$$
(μμ)

and

$$\sigma(x_2,\lambda) = \lambda \qquad (15)$$

It is also assumed that at least wide sense statistical homogeneity prevails. The autocorrelation of stress fluctuations, according to Papoulis (1965) is defined by the formula

$$E\langle \underline{\sigma}(\underline{x}_{1},\lambda)\underline{\sigma}(\underline{x}_{2},\lambda)\rangle = R_{\sigma\sigma}(\underline{x}_{1},\underline{x}_{2},\lambda) = E\langle \lambda^{\bullet}(\underline{x}_{1}),\underline{\bullet}(\underline{x}_{2})\rangle$$

$$= E\langle \underline{\sigma}(\underline{x}_{1},\lambda)\underline{\sigma}(\underline{x}_{2},\lambda)\rangle = R_{\sigma\sigma}(\underline{x}_{1},\underline{x}_{2},\lambda) = E\langle \lambda^{\bullet}(\underline{x}_{1}),\underline{\bullet}(\underline{x}_{2})\rangle \qquad (46)$$

where E denotes the expectation and R is correlation of data. If $x_1 = x + \Delta$ and $x_2 = x$, then

$$E\langle \underline{\sigma}(\mathbf{x} + \Delta, \lambda) \underline{\sigma}(\mathbf{x}, \lambda) \rangle = R_{\sigma\sigma}(\Delta, \lambda) = R_{\sigma}(\Delta, \lambda)$$

$$= E\langle \underline{\sigma}(\mathbf{x} + \Delta) \rangle + \underline{\sigma}(\mathbf{x}) \rangle \qquad (47)$$

From Eq. (43),

$$\underline{\mathbf{m}}(\mathbf{x}) = \ln \underline{\sigma}(\mathbf{x}, \lambda) / \ln \lambda. \tag{48}$$

Hence, the autocorrelation of slope is

$$E'\underline{m}(\mathbf{x}_1)\underline{m}(\mathbf{x}_2)\rangle = R_{\mathbf{x}_1}(\mathbf{x}_1,\mathbf{x}_2,\lambda) = R_{\mathbf{x}_1}(\Delta,\lambda)$$

$$= (1/(\ln \lambda)^2)E(\ln \underline{\sigma}(\mathbf{x}_1,\lambda)\ln \underline{\sigma}(\mathbf{x}_2,\lambda))$$

$$= (1/(\ln \lambda)^2)E(\ln \underline{\sigma}(\mathbf{x}_1+\Delta,\lambda)\ln \underline{\sigma}(\mathbf{x}_2,\lambda)). \quad (49)$$

Letting $\sigma_1 = \sigma(x_1, \lambda)$ and $\sigma^2 = \sigma(x_2, \lambda)$,

$$R_{\sigma}(\Delta,\lambda) = \int_{-\infty}^{\infty} \int_{-\infty}^{\infty} \underline{\sigma}(x_{1},\lambda)\underline{\sigma}(x_{2},\lambda)f_{\sigma_{1}\sigma_{2}}[\underline{\sigma}(x_{1},\lambda)\underline{\sigma}(x_{2},\lambda),\lambda]d\sigma_{1},d\sigma_{2},$$
(50)

where f is the probability density function. Similarly,

$$R_{\mathbf{a}}(\Delta,\lambda) = \int_{-\infty}^{\infty} \int_{-\infty}^{\infty} \underline{m}(x_{1},\lambda)\underline{m}(x^{2},\lambda)f_{\mathbf{a}_{1},\mathbf{a}_{2}}[\underline{m}(x_{1},\lambda),\underline{m}(x_{2},\lambda),\lambda]dm_{1}dm_{2}$$

$$= \int_{-\infty}^{\infty} \int_{-\infty}^{\infty} (1/(\ln \lambda)^{2})\ln [\sigma(x_{1},\lambda)]\ln [\sigma(x_{2},\lambda)]$$

$$\times f_{1}\sigma_{2}[\underline{\sigma}(x_{1},\lambda)\underline{\sigma}(x_{2},\lambda),\lambda]d\sigma_{1}d\sigma_{2} \qquad (51)$$

$$= [1/(\ln \lambda)^{2}]\underline{E}(\ln \underline{\sigma}(x + \Delta,\lambda)\ln \underline{\sigma}(x,\lambda)). \qquad (52)$$

Dividing Eq. (52) by $R_{\bullet}(0,\lambda)$,

$$\frac{R_{\mathbf{n}}(\Delta,\lambda)}{R_{\mathbf{n}}(0,\lambda)} = \frac{\sum_{\mathbf{x}=1}^{\mathbf{n}-\Delta} \ln \underline{\sigma}(\mathbf{x},\lambda) \ln \underline{\sigma} \mathbf{x} + \Delta,\lambda}{\sum_{\mathbf{x}=1}^{\mathbf{n}-\Delta} (\ln \underline{\sigma})^2}$$
 for $\Delta = 1,2...M$

which corresponds to the equation used to determine the autocorrelation in the spectral analysis routine, which will be discussed later.

Since the spectral density $f_T(w)$, of a process x(t) is the Fourier transform of the autocorrelation,

$$\mathbf{f}_{\mathrm{T}}(\omega) = \int_{-\infty}^{\infty} e^{-\mathbf{i}\omega\tau} R(\lambda) d\lambda,$$
 (54)

and since $R(-\lambda) = R(\lambda), f_T(\omega)$ is a real function. Using the Fourier inversion formula

$$R(\lambda) = (1/2\pi) \int_{-\infty}^{\infty} f_{T}(\omega) e^{i\omega\lambda} d\omega, \qquad (55)$$

which yields, with $\lambda = 0$,

$$R(0) = (1/2\pi) \int_{-\infty}^{\infty} f_{T}(\omega) d\omega = E\langle x(t)x(t)\rangle = E\langle [x(t)]^{2}\rangle \ge 0$$
(56)

therefore $f_T(w)$ is non-negative. If x(t) is real, then $R(\lambda)$ is real and even, and $f_T(w)$ is also even and Eq. (54) and (55) can be written

$$f_{T}(\omega) = \int_{-\infty}^{\infty} \Re(\lambda) \cos \omega \lambda \, d\lambda$$
 (57)

and

$$R(\lambda) = (1/2\pi) \int_{-\infty}^{\infty} f_{T}(\omega) \cos \omega \lambda \, d\omega \qquad (58)$$

In this investigation the interest is mainly in the first and second moments,

$$\langle \underline{\underline{K}}(\underline{x},t) \rangle = \int_{-\infty}^{\infty} \underline{\underline{K}}(\underline{x},t) dP[\underline{\underline{K}}(\underline{x},t)],$$
 (59)

and

$$\langle \underline{\underline{K}}(\underline{x}_1,t)\underline{\underline{K}}(\underline{x}_2,t)\rangle = \int \underline{\underline{K}}(\underline{x}_1,t)\underline{\underline{K}}(\underline{x}_2,t) d\underline{\underline{K}}(\underline{x}_1,\underline{x}_2,t)],$$
(60)

Eq. (59) being written in the general form of a correlation.

It would be expected that a spectral tensor could be found which is a Fourier transform of the correlation tensor,

$$\underline{\underline{\bullet}}(\underline{\omega},t) = 1/8\pi^3 \int_{-\infty}^{\infty} \underline{\underline{R}}(\underline{x}_1 - \underline{x}_2,t) e^{i\underline{\omega}\underline{x}} d\underline{x}.$$
 (61)

V. EXPERIMENTAL INVESTIGATION

Greenhouse-grown, Vernal alfalfa was used in this investigation.

Two stems were used for the cross-sectional area analysis and one of these two stems was used for the relaxation studies. Table 1 lists the internodal distances for the two stems, with stem 2 used for the relaxation studies.

Table 1. Internodal distances of two alfalfa stems used for area and relaxation characteristic fluctuations.

	Distance above gr	cound level, cm
Location	Stem 1	Stem 2
First node	12.1	8.1
Second node	24.2	16.7
Third node	36.9	26.2
Fourth node	1.7 7	3 9.5
Fifth node	56.3	50.9
Sixth node	62.3	61.1
Seventh node	67.4	67.4
Eighth node	71.8	70 .2
Top	78.1	76.6

The portion of the stem from one and one-half inches above ground to about the fifth node was used for sectioning and subsequent studies.

Other nodes existed between number eight and the top, but were not recorded.

Ten other alfalfs stems, three through 12, were harvested the same day as stems 1 and 2 and used for area determination comparisons. The internodal distances for the ten stems are shown in Table 2. Other nodes existed between number and nine and the top but were not recorded.

Table 2. Internodal distances of alfalfa stems used for area determination comparisons

			Dist	ance a	ibo ve g	round	level,	cm		
		Stem Designation								
Location	3	4	5	6	7	8	9	10	11	12
First node	8.9	8.9	4.5	3.8	5.7	4.5	3.2	2.5	5.1	2.5
Second node	17.8	17.7	12.7	12.7	15.3	15.3	10.8	11.4	14.1	13.9
Third node	28.1	28.4	2 5.4	22.2	28.4	25.14	24.8	21.1	27.2	24.7
Fourth node	38.2	35.6	34.2	30.5	38.1	35.6	34.7	31.2	39.2	36.2
Fifth node	145.7	111.3	1,0.9	36.9	144.3	45.7	44.1	41.7	47.1	47.2
Sixth node	52.1	1,8.9	1,8.2	41.3	50.8	53.4	46.6	50.4	52.2	54.6
Seventh node	58.4	54.1	54.6	47.1	54.5	59.7	53 .3	57.7	55.2	61.1
Eighth node	65.4	59 .2	59.6	53.2	58.8	67.3	57.4	64.8	59.7	66.3
Ninth node	70.6	63.5	63.6	57.8	63.6	72.4	62.2	72.2	64.1	73.7
Тор	78.7	76.9	77.5	78.5	78 .7	81.4	77.4	76.4	78.8	82.1

The 12 stems were dried by exposing them to ambient conditions for one week and then placed in a darkened cabinet until needed. The ambient conditions (75°F d.b. and about 30% RH) were such that the moisture content of the stems was main tained at eight percent (wet basis) during storage and subsequent testing.

A. Area Measurement

One of the more difficult problems involved in working with the physical properties of forages has been determining the area upon which stresses have been applied. To further complicate matters, alfalfa stems are usually hollow and take the shape of four-sided irregular polygons.

Several researchers have simplified their approach to the area determination problem by assuming that alfalfa stems are round and performing a measurement which they call a "diameter," and then base their subsequent calculations on this "diameter." The validity of the results is dependent on the "correctness" of the "diameter" measurement and is not known. Halyk (1962) used a "shadow box" arrangement which consisted of a box which had provisions for controlled illumination, and used photographic paper upon which alfalfa stems were placed for exposure. The "diameter" of the stem was estimated on the exposed photographic paper. The results based on this method could vary considerably depending upon the stalk orientation. Prince (1965) used a micrometer to measure the outside "diameter" of alfalfa stems. Both Halyk (1962) and Prince (1965) neglected the hollow characteristic of alfalfa stems. Bhan (1959), in conducting research concerning exposed area drying rates of alfalfa, assumed an outside and inside "diameter" and calculated the exposed areas based on these "diameters."

The cross-sectional area measurements for this study were made by photographing cross-sectional views of short sections of alfalfa stems on 35 mm film (examples of several sections are shown in Figure 4) and measuring the resultant image areas on the film negatives with a Flying-Spot Particle Analyzer (FSPA), shown in Figure 5. The FSPA has two main systems: a flying-spot film scanner and a set of logic circuits comprising a special purpose computer. A cathode-ray tube generates a moving spot of light which scans across the film field in raster fashion. The image-modulated light beam transmitted by the test film is collected by a condenser lens and directed to a multiplier phototube. The output of the phototube goes to the preemplifier, amplitude threshold quantizer, and on to the computing circuits which perform various preselected measurement calculations. A block diagram of the flying-spot film scanner is shown in Figure 6a. The FSPA circuits are shown in Figure 6b.

An area measurement is made by measuring the total length of scans across the particles. The length is obtained with the aid of a two-megacycle crystal oscillator, located in the display counter, from which pulses are routed to the display counter by logic gate circuits. The intercept pulses, occurring when the scan spot crosses a boundary of the particles, are used to gate the display counter, to start and stop it, thereby totalizing the clock-pulse elements for all the intercepts.

High-contrast copy film manufactured by Eastman Kodak, with an ASA rating of 64 was used for the negatives of cross-sectional areas to be scanned on the FSPA. The developing recommendations of Kodak were followed. The light transmission through the processed negatives was as follows: film background, three percent; and through the solid portion of the stem cross-section, 78 percent. The light transmission was

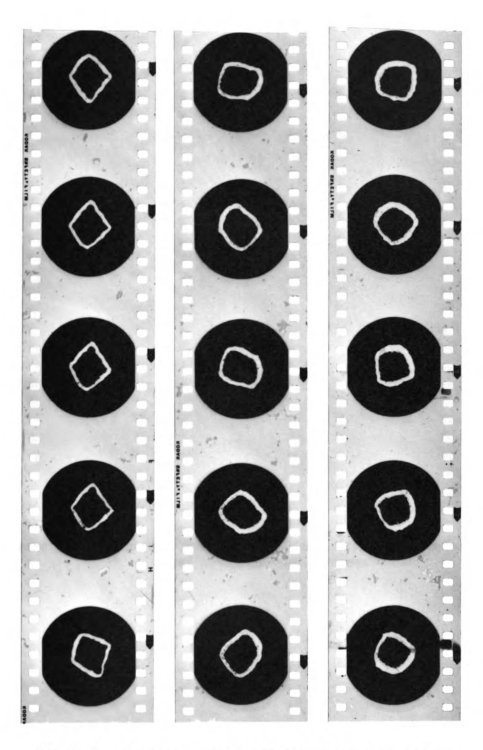


Figure 4. Examples of film negatives of stem crosssectional views as used in Flying-Spot Perticle Analyzer for area measurement

Figure 5. Flying-Spot Particle Analyzer used to determine area cross-sectional areas

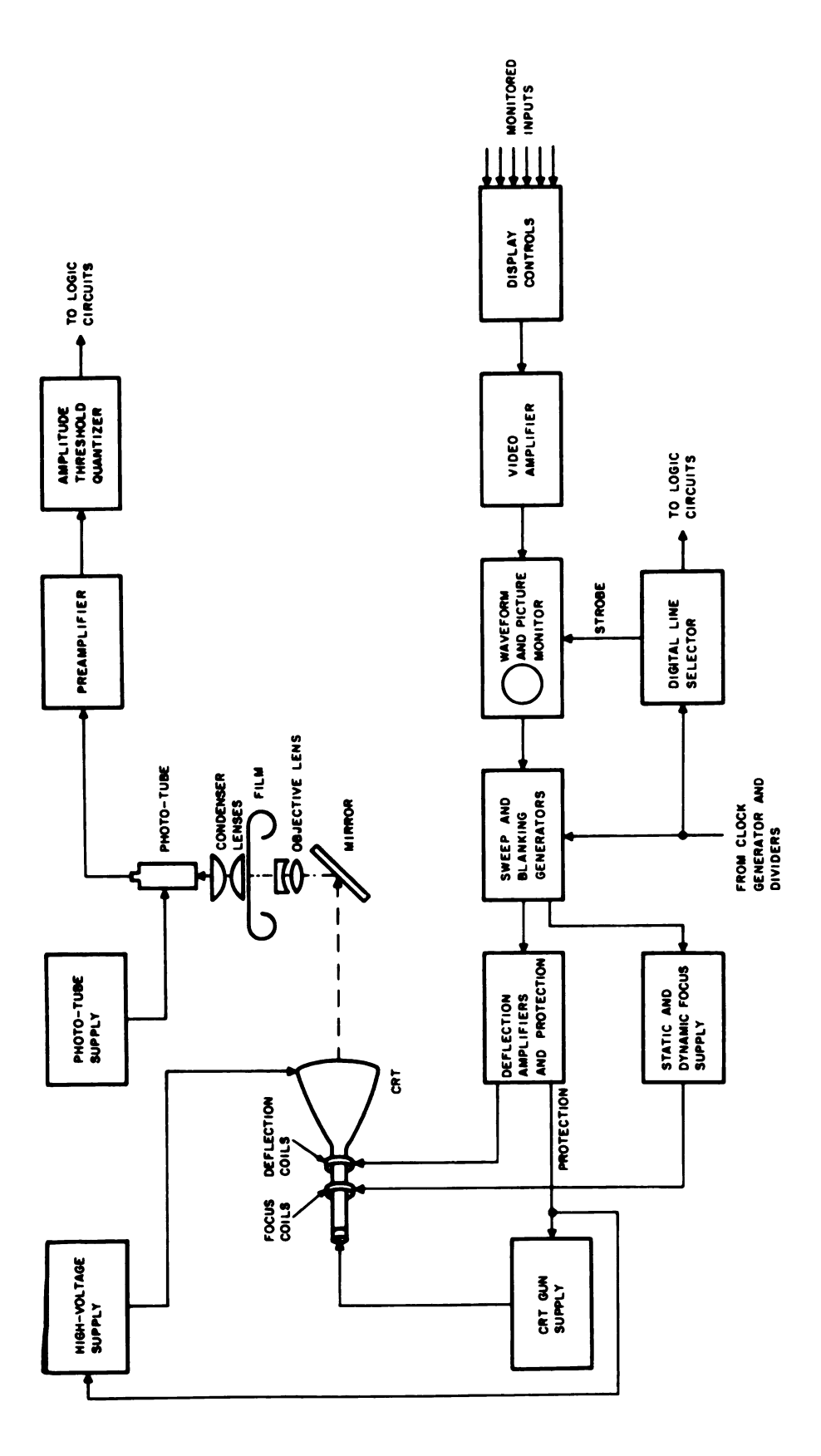
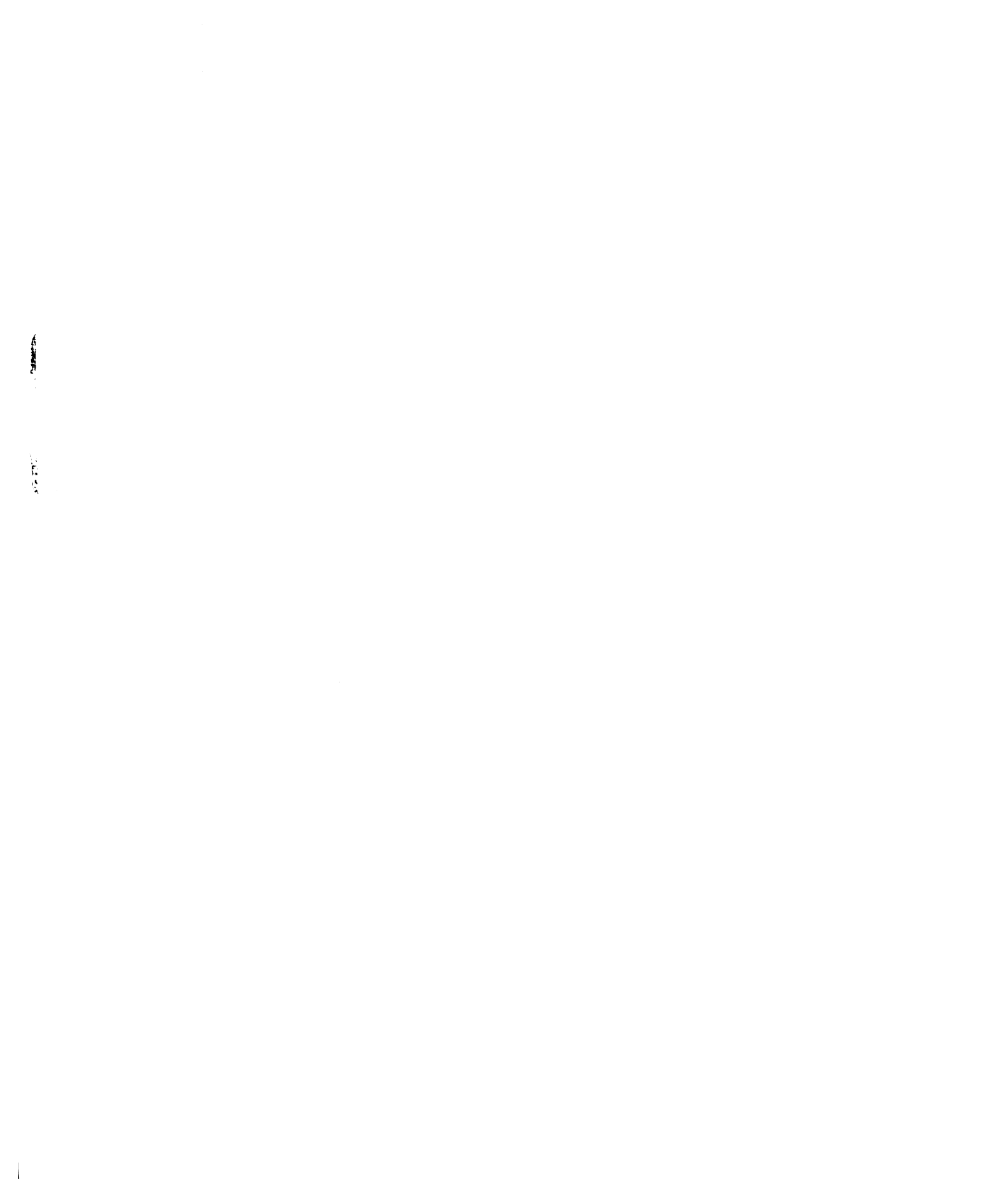


Figure 6a. Block diagram of Flying-Spot Particle Analyzer film scanner



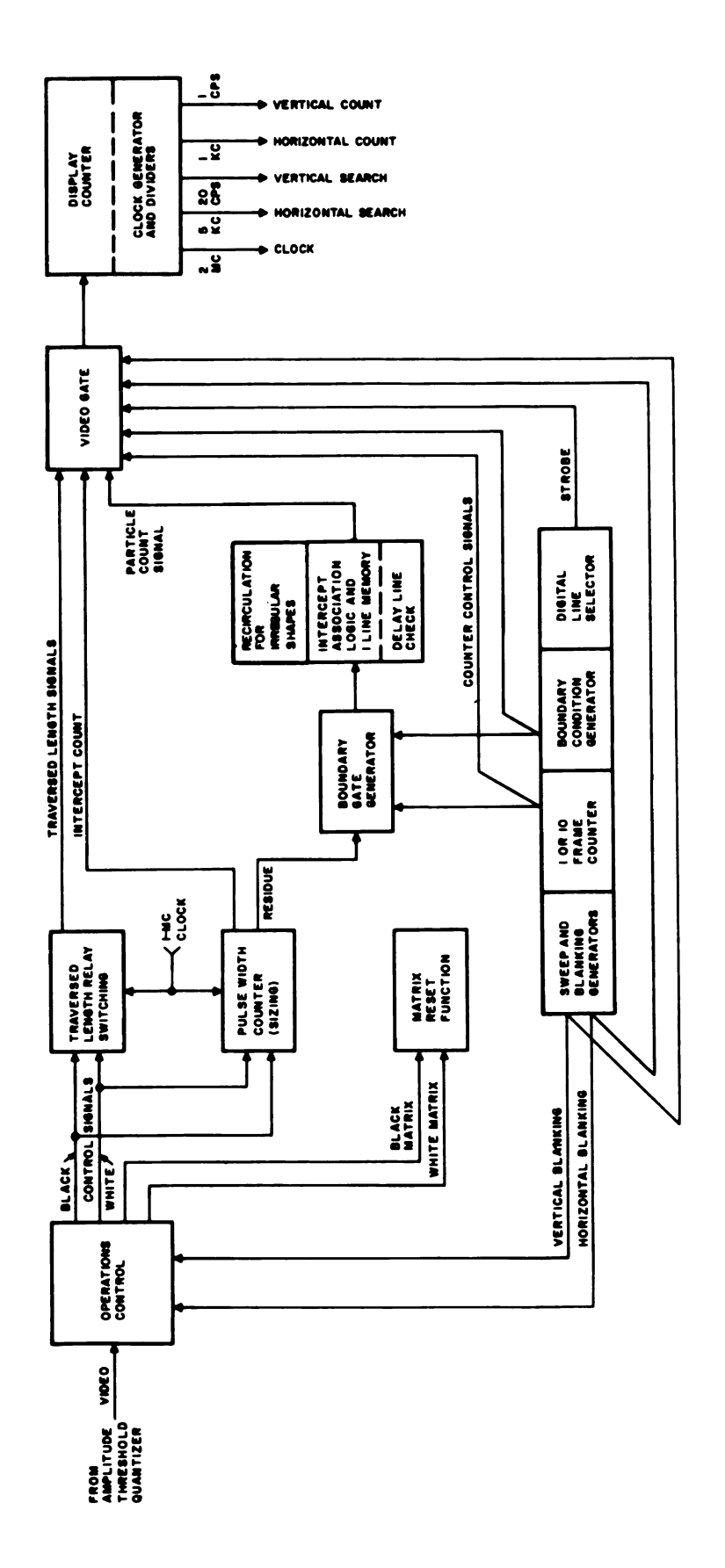


Figure 6b. Block diagram of Flying-Spot Particle Analyzer logic circuits

measured with the Flying-Spot Particle Analyzer (FSPA) with the 100 percent transmission base taken as the light transmitted through the area between frames which had not been exposed to light prior to film development. The background film density was maintained constant by using an exposure meter adapted to the microscope to determine the proper exposure settings on the 35 mm camera for each and every cross-sectional stem area photographed.

The area data were automatically punched on standard computer input cards for use in the spectrum analysis of the area data and subsequent stress calculations for the relaxation experiments.

The stem sections were prepared by cutting the stem on a high-speed cut-off saw shown in Figure 7. The air-powered saw, with a one-inch diameter 70-tooth blade, turned at approximately 65,000 rpm. A set-screw adjustment permitted cutting a consistent section length of 0.75 mm. The saw blade cut was 0.25 mm thick resulting in area measurements taken at intervals of one mm. The stem sections were photographed on 35 mm high-contrast copy film immediately after sectioning and were maintained in order of cutting throughout the experiment. The orientation of the sections was maintained to assure that the photographs were taken at one mm intervals along the stem.

In an attempt to compare cross-sectional areas of alfalfa stems obtained by several methods, areas were determined with a micrometer "diameter" measurement, a microscope "diameter" measurement, and the FSPA area measurement.

Ten stems similar to the two used for the area spectrum work and relaxation tests were selected and measured at the midpoint between nodes with a micrometer to determine the distance between opposite flat

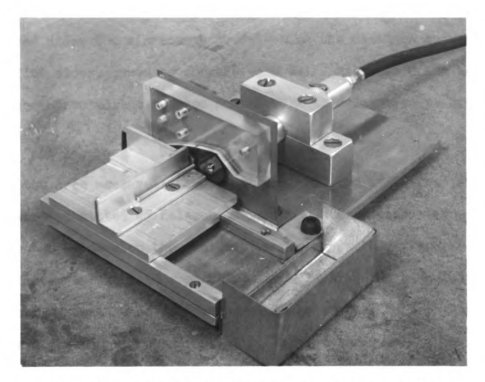


Figure 7. Cut-off saw used to section alfalfa stems



Figure 8. Device for conducting relaxation experiments of alfalfa stem sections

sides. A cross-section was then removed at the midpoint between nodes and measured under the microscope to determine the distance between opposite flat sides, opposite corners, and wall thickness. The section was then photographed and scanned on the FSPA to determine its area.

B. Relexation Tests

Afer the area measurements were determined, the individual stem sections were submitted to relaxation tests. Supplementary tests, which were conducted to develop the equipment, were run with a standard four-inch micrometer as the main support member. Further tests indicated the need for strengthening the main support member and the device shown in Figure 8 evolved and was used for all relaxation tests.

A relaxation test was conducted by placing the stem section vertcally on the load cell of the relaxation test stand. A piece of brass
shim stock was placed on top of the specimen and firmly held to prevent
twisting of the specimen as the load was applied. The load was applied
to the section manually by turning the micrometer screw down onto the
shim stock and alfalfa stem section until the desired load was applied
as registered on a recording oscillograph chart via the load cell. A
stress of 3,000 grams per square millimeter (gsmm) was applied to each
section. Approximately 6,000 gsmm were required to collapse the section.
The deflection required to achieve a stress of 3,000 gsmm was held constant during the 200-second relaxation test. The 3,000 gsmm stress
level was selected to assure that the complete set of relaxation tests
could be conducted at a common stress.

Tests conducted by placing the stem section horizontally on the load cell, with the stem sides collapsed, yielded stress relaxation curve slopes that were twice those of stems tested vertically. As a result of this, all subsequent tests were conducted with the stem section placed vertically on the load cell since this was the direction that exhibited the greater, or limiting, strength if the stems were under compression.

Figure 9 shows two of the relaxation curves obtained.

The load exerted on the alfalfa stem section was monitored by the differential transformer load cell which transmitted an electrical signal to the recorder where the signal was amplified and recorded. A curve reader coupled to a card punch was used to read points on the curves and punch the data on card for further analysis on an IEM 1620 computer.

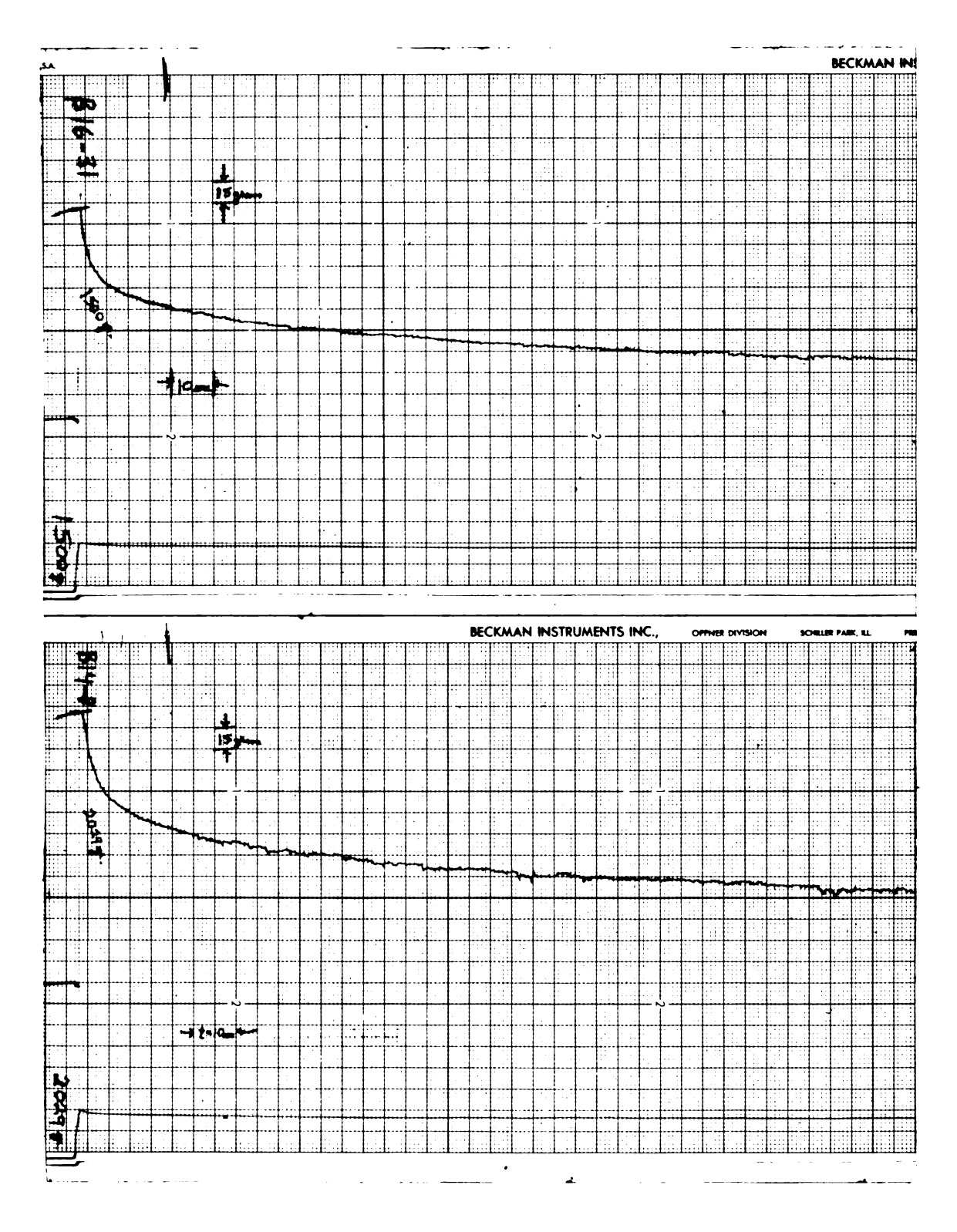


Figure 9. Two stress relaxation curves obtained during the investigation

VI. RESULTS AND DISCUSSION

A. Comparison of Area Measurement Methods

The comparison of cross-sectional area measurements made by several methods is given in Table 3. The Flying-Spot Particle Analyzer (FSPA) measurement was determined as previously described. The microscope measurement was made by measuring the distance across opposite sides of the alfalfa stem at their midpoints and measuring the wall thickness of the stem section. These measurements were made on the stem while it was in position for photography as utilized in the FSPA method. The microscope measurements were made with a micrometer scale in the microscope ocular.

Prior to stem sectioning for the FSPA and microscope measurements, a micrometer was used to measure across opposite sides of the alfalfa stem at the location of the section to be removed. Distances A and B were the longer and shorter distances across the stem sides. AxB would assume that the stem is a rectangle A units long and B units wide; $\pi A^2/4$ and $\pi B^2/4$ assumes a round stem configuration with a diameter of A and B respectively; and $\pi (A+B)^2/16$ assumes a round stem configuration with a diameter of (A+B)/2. None of the micrometer measurements took into consideration the fact the stem was hollow.

The section designation used in Table 3 indicates the stem number, from three to twelve corresponding to Table 2 internodal distances, followed by the two numbers which designate the two nodes between which the section was measured.

Table 3. Comparison of cross-sectional area measurements

	Cross-sectional area, mm ²									
Section		Micro- scope	Micrometer							
	FSPA		AxB	πA ² /4	πB ² / 4	$\pi(A+B)^2/16$				
101	0.417	0.74	1.86	2.28	0.94	1.54				
112	0.711	0.97	2.18	2.86	1.02	1.94				
123	0.3 54	0.78	1.94	1.65	1.42	1.54				
134	0.214	0.62	1.68	1.42	1.22	1.32				
145	0.430	0.59	3.87	1.42	1.22	1.32				
156	0.215	0.64	1.55	1.27	1.17	1.22				
167	0.249	0.63	1.48	1.22	1.12	1.17				
178	0.499	0.54	1.42	1.22	1.02	1.12				
189	0.263	0.44	1.01	0.81	0.77	0.79				
201	0.450	1.05	1.61	1.32	1.22	1.27				
212	0.474	0.96	2.36	1.94	1.75	1.85				
223	0.843	1.11	2.21	1.75	1.71	1.73				
234	0.575	0.85	1.94	1.65	1.42	1.54				
245	0.577	0.84	2.03	1.75	1.42	1.59				
256	0.437	0.71	1.84	1.54	1.37	1.46				
267	0.505	0.50	1.33	1.07	1.02	1.05				
278	0.321	0.38	1.30	1.22	0.85	1.03				
289	0.351	0.29	0.86	0.70	0.65	0.68				
301	0.715	1.18	1.42	1.27	0.98	1.13				
312	0.788	1.08	1.64	1.37	1.22	1.30				
323	0.766	0.99	2.13	1.95	1.40	1.68				
			2.72	2.34	1.95					
334 21.5	0.916	1.39				2.15				
345	1.046	1.07	2.52	2.01	1.95	1.98				
356	0.725	1.08	1.92	1.54	1.48	1.51				
367	0.618	0.79	1.46	1.16	1.12	1.14				
378	0.602	0.85	1.55	1.32	1.12	1.22				
389	0.521	0.62	1.41	1.30	0.94	1.12				
412	0.924	1.65	2.29	1.83	1.77	1.80				
423	0.818	1.52	2.56	2.01	2.01	2.01				
434	0.751	1.46	2.68	2.15	2.07	2.11				
445	0.885	1.44	2.77	2.21	2.15	2.18				
456	0.798	1.21	2.55	2.15	1.89	2.02				
467	0.725	1.27	2.32	1.89	1.77	1.83				
478	0.792	0.92	1.84	1.48	1.43	1.46				
489	0.455	0.67	1.52	1.22	1.17	1.19				
501	1.150	1.74	2.56	2.07	1.95	2.01				
512	0.907	1.59	2.77	2.21	2.14	2.18				
523	0.740	1.59	2.98	2.49	2.21	2.35				
534	1.100	1.51	3.12	2.49	2.42	2.45				
545	1.011	1.64	2.94	2.3 5	2.28	2.32				
556	0.881	1.38	2.32	1.89	1.77	1.82				
567	0.959	1.50	2.48	2.09	1.82	1.96				
578	0.763	1.06	2.40	2.01	1.77	1.89				
589	0.915	1.02	2.13	1.77	1.59	1.68				

(Table No. 3 Continued)

601 612 623 634 645 656	1.025 0.862 0.793 0.619 0.407 0.559 0.367	1.60 1.16 0.91 1.09 0.95 1.14 0.82	2.32 2.40 2.64 2.48 2.64 2.40	1.83 1.89 1.89 2.08 1.95 2.08 1.89	1.83 1.77 1.89 2.08 1.95 2.08 1.89	1.83 1.82 1.89 2.08 1.95 2.08 1.89
678 689	0.464 0.499	0.84 0.69	2.43 2.07	2.14 1.65	1.71 1.54	1.92 1.59
712	1.281	1.86	3.29	2.85	2 .3 5	2.60
723	1.075	1.67	3.30	2.71	2.49	2.60
734	1.068	1.62	3.05	2.49	2.35	2.62
745	0.898	1.34	2.48	2.08	1.83	1.96
756	0.983	1.03	1.88	1.59	1.37	1.48
767	0.788	0.89	1.91	1.65	1.37	1.51
778 780	0.780	0.85	1.74	1.43	1.32	1.37
789	0.571 0.635	0.85 1.17	1.55 1.88	1.22 1.49	1.22 1.49	1.22 1.49
812 823	0.683	0.97	2.08	1.95	1.37	1.66
834	0.612	1.01	2.17	1.83	1.59	1.71
845	0.577	0.99	1.88	1.54	1.42	1.48
856	0.374	0.90	1.81	1.48	1.38	1.43
867	0.279	0.76	1.81	1.48	1.38	1.43
878	0.179	0.64	1.52	1.22	1.17	1.20
889	0.303	0.36	1.48	1.17	1.17	1.17
901	0.891	1.60	2.08	1.77	1.54	1.65
912	0.868	1.32	2.17	1.83	1.59	1.71
923	0.873	1.31	2.40	1.95	1.83	1.89
934	0.876	1.57	3.05	2.49	2.35	2.42
945	1.007	1.46	2.61	2.08	2.02	2.05
956 957	0.834	1.16	2.27	1.89	1.71	1.80
967 078	0.615	1.02 0.63	3.23	1.37 1.27	1.17	1.27 1.17
978 989	0.405 0.314	0.53	1,48 1,20	0.98	1.08 0.90	0.94
1012	0.822	1.10	2.23	2.28	1.59	1.94
1023	0.619	1.21	2.56	2.01	2.01	2.01
1034	0.479	1.06	2.93	2.49	2.14	2.32
1045	0.504	0.88	2.56	2.21	1.83	2.02
1056	0.790	0.77	2.47	1.95	1.95	1.95
1067	0.545	0.90	2.39	2.08	1.72	1.90
1078	0.540	0.80	2.10	1.65	1.65	1.65
1089	0.750	0.68	1.74	1.48	1.27	1.37

Se an

```
Parzen Spectrum
Dimension X(1000),C(101),V(101),SQ(101)
С
                              Begin Trace
                                                                                               Parameter Card
          1 kead 501,1D,N,K
501 Format(215,14)
                             ISN=0
             ISN=0

IF (N-K)99,99,51

51 IF (N-1000)10,10,99

10 IF (K-101)11,11,99

READ UP TO 100 DATA CARDS

11 NC=(N+9)/10
                           NC=(N+9)/10

DO 2 J=1,NC

J1=1+((J-1)*10)

J2=1+((J-1)*10)

J3=1+((J-1)*10)

J4=1+((J-1)*10)

J5=1+((J-1)*10)

J7=1+((J-1)*10)

J8=1+((J-1)*10)

J9=1+((J-1)*10)

J10=1+((J-1)*10)

REAU 502, JD.ICN X
         J10=1+((J-1)+10)
READ 502, JD, ICN, X(J1), X(J2), X(J3), X(J4), X(J5),
1X(J6), X(J7), X(J8), X(J9), X(J10)
502 FORMAT(215, 10F7.0)
IF(ID-JD)98,12,98
12 IF(ICN-ISN)98,98,13
13 ISN-ICN
                    2 CONTINUE
                                      COMPUTE SSQ+SXP
                             SXX=0.0
                              DO 45 J=1,N
              45 SXX=SXX+(X(J)+X(J))
                             DO 44 J=1,K
                             SXP=0.0
                             N5=N-J
                             N6-N5+1
                              DO 5 I=1,N5
                              JJ=Í+J
                  5 SXP=SXP+(X(I)+X(JJ))
SXX=SXX-(X(N6)+X(N6))
C(J)=SXP/SXX
              此 SQ(J)=SXX
                                     COMPUTE SPECTRAL DENSITY FOR FREQUENCY W
                             CK-K
                             DO 8 J-1,K
                             SCQ=0.0
                             CJ=J
                              CJK-CJ/CK
                              DO 7 I-1,K
                              CI=I
                              CR=CI/CK
             IF(CR-0.5)\[\bar{1}\bar{6}\],\[\bar{1}\bar{6}\],\[\bar{1}\bar{6}\],\[\bar{1}\bar{6}\],\[\bar{1}\bar{6}\],\[\bar{1}\bar{6}\],\[\bar{1}\bar{6}\],\[\bar{1}\bar{6}\],\[\bar{6}\],\[\bar{6}\],\[\bar{6}\],\[\bar{6}\],\[\bar{6}\],\[\bar{6}\],\[\bar{6}\],\[\bar{6}\],\[\bar{6}\],\[\bar{6}\],\[\bar{6}\],\[\bar{6}\],\[\bar{6}\],\[\bar{6}\],\[\bar{6}\],\[\bar{6}\],\[\bar{6}\],\[\bar{6}\],\[\bar{6}\],\[\bar{6}\],\[\bar{6}\],\[\bar{6}\],\[\bar{6}\],\[\bar{6}\],\[\bar{6}\],\[\bar{6}\],\[\bar{6}\],\[\bar{6}\],\[\bar{6}\],\[\bar{6}\],\[\bar{6}\],\[\bar{6}\],\[\bar{6}\],\[\bar{6}\],\[\bar{6}\],\[\bar{6}\],\[\bar{6}\],\[\bar{6}\],\[\bar{6}\],\[\bar{6}\],\[\bar{6}\],\[\bar{6}\],\[\bar{6}\],\[\bar{6}\],\[\bar{6}\],\[\bar{6}\],\[\bar{6}\],\[\bar{6}\],\[\bar{6}\],\[\bar{6}\],\[\bar{6}\],\[\bar{6}\],\[\bar{6}\],\[\bar{6}\],\[\bar{6}\],\[\bar{6}\],\[\bar{6}\],\[\bar{6}\],\[\bar{6}\],\[\bar{6}\],\[\bar{6}\],\[\bar{6}\],\[\bar{6}\],\[\bar{6}\],\[\bar{6}\],\[\bar{6}\],\[\bar{6}\],\[\bar{6}\],\[\bar{6}\],\[\bar{6}\],\[\bar{6}\],\[\bar{6}\],\[\bar{6}\],\[\bar{6}\],\[\bar{6}\],\[\bar{6}\],\[\bar{6}\],\[\bar{6}\],\[\bar{6}\],\[\bar{6}\],\[\bar{6}\],\[\bar{6}\],\[\bar{6}\],\[\bar{6}\],\[\bar{6}\],\[\bar{6}\],\[\bar{6}\],\[\bar{6}\],\[\bar{6}\],\[\bar{6}\],\[\bar{6}\],\[\bar{6}\],\[\bar{6}\],\[\bar{6}\],\[\bar{6}\],\[\bar{6}\],\[\bar{6}\],\[\bar{6}\],\[\bar{6}\],\[\bar{6}\],\[\bar{6}\],\[\bar{6}\],\[\bar{6}\],\[\bar{6}\],\[\bar{6}\],\[\bar{6}\],\[\bar{6}\],\[\bar{6}\],\[\bar{6}\],\[\bar{6}\],\[\bar{6}\],\[\bar{6}\],\[\bar{6}\],\[\bar{6}\],\[\bar{6}\],\[\bar{6}\],\[\bar{6}\],\[\bar{6}\],\[\bar{6}\],\[\bar{6}\],\[\bar{6}\],\[\bar{6}\],\[\bar{6}\],\[\bar{6}\],\[\bar{6}\],\[\bar{6}\],\[\bar{6}\],\[\bar{6}\],\[\bar{6}\],\[\bar{6}\],\[\bar{6}\],\[\bar{6}\],\[\bar{6}\],\[\bar{6}\],\[\bar{6}\],\[\bar{6}\],\[\bar{6}\],\[\bar{6}\],\[\bar{6}\],\[\bar{6}\],\[\bar{6}\],\[\bar{6}\],\[\bar{6}\],\[\bar{6}\],\[\bar{6}\],\[\bar{6}\],\[\bar{6}\],\[\bar{6}\],\[\bar{6}\],\[\bar{6}\],\[\bar{6}\],\[\bar{6}\],\[\bar{6}\],\[\bar{6}\],\[\bar{6}\],\[\bar{6}\],\[\bar{6}\],
                             GO TO 71
              49 CC=1.0-CR
                             CL=2.0#CC#CC#CC
         71 CCOS=COSF(3.1\15927*CI*CJK)
7 SCQ=SCQ=(CL*C(I)*CCOS)
V(J)=.15915508+(SCQ/3.1\15927)
W=CJ/(2.0*CK)
8 FUNCH 50\,ID,N,J,W,SQ(J),C(J),V(J)
50\,FORMAT(315,F7.\,1,3E16.8)
              GO TO 1
99 PRINT 503,N,K
          503 FORMAT(19H PARAMETER INCORRECT, 215)
                              PAUSE
                              GO TO 1
               98 PRINT 505, JD, ICN
          505 FORMAT(9HIDENT ERR, 215)
                              PAUSE
                              GO TO 1
                              END TRACE
                             END
```

The FSPA and microscope methods for cross-sectional area determination take into account the hollowness of the alfalfa stem. It is virtually impossible to accurately measure the stem wall "average" thickness and to allow for the fluctuations that exist. The tendency is to overestimate the wall thickness and, accordingly, to overestimate areas as much as two or three times compared to the areas determined on the FSPA. The microscope area determination was about 50 percent greater, on the average, than the FSPA area measurement.

The micrometer measurement, which failed to take into account the area hollowness, resulted in still greater inaccuracies of cross-sectional area measurements. The AxB determination, which assumes a solid rectangular cross-section, resulted in area measurements about 3.5 times larger than the FSPA measurements. The $\pi A^2/\mu$ and $\pi B^2/\mu$ measurements, which assume a solid round cross-section, resulted in area measurements three and two and two-thirds times, respectively, larger than the FSPA measurement. As would be expected, the measurement with the assumed "diameter" as the average of the two measurements, A and B, resulted in an area two and one-third times the FSPA area measurement.

Inspection of the data reveals that considerable fluctuation occurs in the relationship between FSPA and the microscope and micrometer methods of area determination from section to section. If the other methods of measurement were consistent multiples of the FSPA, it would be a simple matter to correct for inaccuracies, but such is not the case since factors as high as six or as low as one occur randomly. The problems encountered by many researchers in trying to obtain consistent results

when studying forage mechanical properties may be partially attributable to the difficulty in determining the cross-sectional area upon which the load was applied.

B. Method of Analysis

The spectral density and correlation of the cross-sectional area and relaxation curve slope data were determined by methods outlined in Blackman and Tukey (1958). Several changes in the methods suggested by Mennell and Turney (1965) were incorporated into the IBM 1620 computer program, shown in Table 4. The Blackman and Tukey (1958) version uses autocovariance to calculate the spectral density rather than the normalized correlation coefficient.

The first step in the calculation of spectral density and correlation of data is to form the sample autocovariance for lag period v, and N pieces of data.

$$R(v) = (1/N) \sum_{t=1}^{N-v} X(t)x(t+v), \text{ for } v = 0,1,w, ... M$$
 (62)

and the sample autocorrelation coefficient for lag v

$$\rho(v) = R(v)/R(0) = \sum_{t=1}^{N-v} x(t)x(t+v)/\sum_{t=1}^{N-v} x^{2}(t), \text{ for } v = 0,1,2 \dots M$$
(63)

Autocovariance and autocorrelation are analogous to the sums of squares and correlation coefficient, respectively. However, the calculations are performed on all pairs of data with a difference of v periods. When R(v), the autocovariance, or $\rho(v)$, the autocorrelation (normalized version of R(v)) are analyzed, relatively high absolute values indicate higher correlation between the t and t + v terms.

The contribution of each lag (frequency) is determined by calculating the spectral density. We determine this by the equation

$$f_{T}(\omega) = (1/2\pi)\rho(0) + (1/\pi) \sum_{v=1}^{M} \lambda_{v} \cos(\pi k v/Q)\rho(v)$$
 (64)

where M is the truncation point of the calculations and $\lambda_{_{\mbox{\scriptsize V}}}$ is the Parzen lag window which is evaluated as follows:

$$\lambda_{v} = 1 - 6(v/M)^{3}, \quad \text{for } v/M \le 0.5$$

$$= 2(1 - (v/M))^{3}, \quad \text{for } 0.5 \le v/M \le 1.0$$
(65)

The spectral density is obtained by representing the autocorrelation as the Fourier transform. By inversion the spectral density is expressed as a function of the autocorrelation. The frequency, ω , is equal to K/2Q where K denotes the computation interval, $K = 1, 2, \ldots Q$.

C. Area Spectral Density and Correlation

The cross-sectional area spectral density (power spectrum) analysis involved removing the trend of decreasing area from bottom to top of the alfalfa stem. This was done by analyzing the raw data and determining empirically the equation which best described the trend of area change. Obviously, if enough terms were used in the trend equation all fluctuation would be eliminated and a spectrum analysis would not needed. First order equations seemed to adequately describe the trend of the two stems and were used to remove trends from the data.

After the trend was removed the two stems were treated as one continuous stem for the spectrum analysis. One thousand area determinations were included in the analysis.

The spectral density and correlation of the stem area data are shown in Figure 10. Both the spectral density and correlation curves tend to describe the area fluctuations and serve as a check on each other. The correlation data have been normalized and the reading at zero mm would be unity since the correlation between two measurements at the same location would be unity. As the area measurements were made at greater distances from each other the correlation decreases rapidly. As a result, if area measurements are not determined at or within 0.75 mm of the point of load application considerable error may exist between what was analyzed and what someone thought was analyzed.

Another useful function of the spectral density analysis would be to determine the validity of proposed growth models of biological substances. If alfalfa stem growth was hypothesized in a certain way the cross-sectional area data, which certainly reflects growth, would be a type of data to analyze to check the validity of the growth model.

D. Relaxation Spectral Density and Correlation

The data obtained from the relaxation curves were of the mathematical form

$$\ln \sigma(t) = m \ln t - m \ln t_0 + \ln \sigma_0.$$
 (66)

Letting A = -m ln t_0 + ln σ_0 , and B = m, the slope of the curve in Eq. (66) we get

$$\ln \sigma(t) = A + B \ln t, \qquad (67)$$

the form of the equation used to describe the relaxation data of the alfalfa stem sections. The selection of the equation form was verified by submitting the relaxation data to a curve-fitting routine on an IBM 1620

•

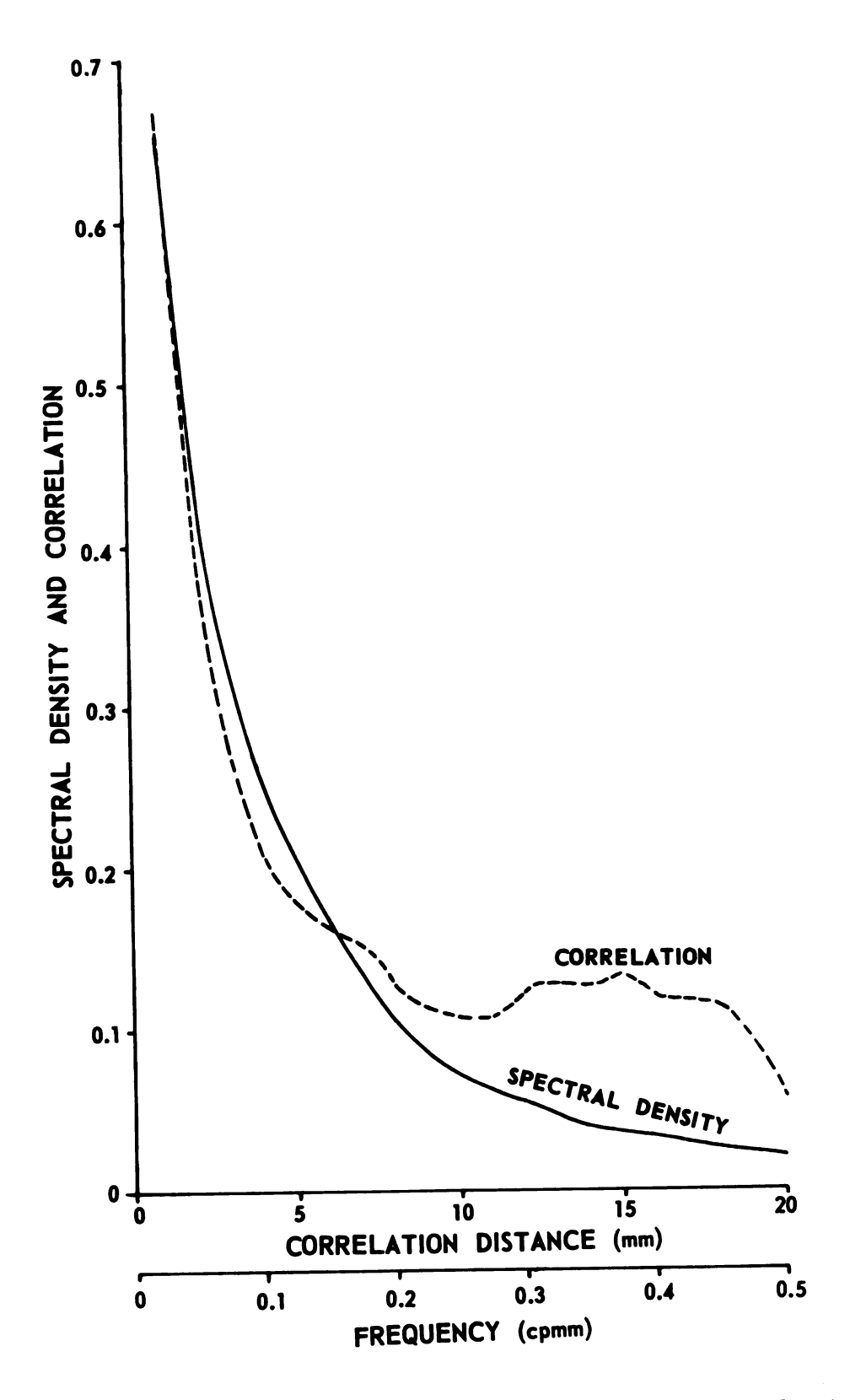


Figure 10. Spectral density and correlation and alfalfa stem cross-sectional areas

computer using various equation forms. The R-values, which indicate the closeness of fit for the actual data points to the selected equation were very close to unity, an R-value of one indicating, of course, a very close fit.

Inspection of the data indicated that it was not necessary to remove a trend from the data prior to analysis. The parameter selected for analysis was the coefficient B, the slope of the relaxation curves. A series of 540 relaxation experiments were conducted. The mean values of A and B for the 540 relaxation tests were 8.003414 and -0.010731, respectively, with standard deviations of 0.002724 and 0.003716.

The spectral density and correlation of the relaxation curve slopes are shown in Figure 11. Since the correlation data are normalized the value is unity at zero mm. The correlation coefficient was 0.9 or slightly higher for the 100 mm lag under consideration, indicating that the location selected to remove a section for testing is not critical, at least within a 100 mm span. The area to be measured for this test section, as previously noted, must be selected carefully.

The spectral density curve is essentially flat from about 0.1 cpmm out to 0.5 cpmm. The peak at 0.025 cpmm indicates that a large non-zero mean component may be present at zero cpmm and the contribution is so large that it affects the very low frequencies. In order to further analyze the very low frequencies we would need considerably more data. Since we are dealing with a finite structure, we can never get an infinite number of data points. We can, however, pool the data from more stems to resolve the lower frequencies. Unfortunately we would probably introduce periodicities at the end of stems and fail to resolve the problem.

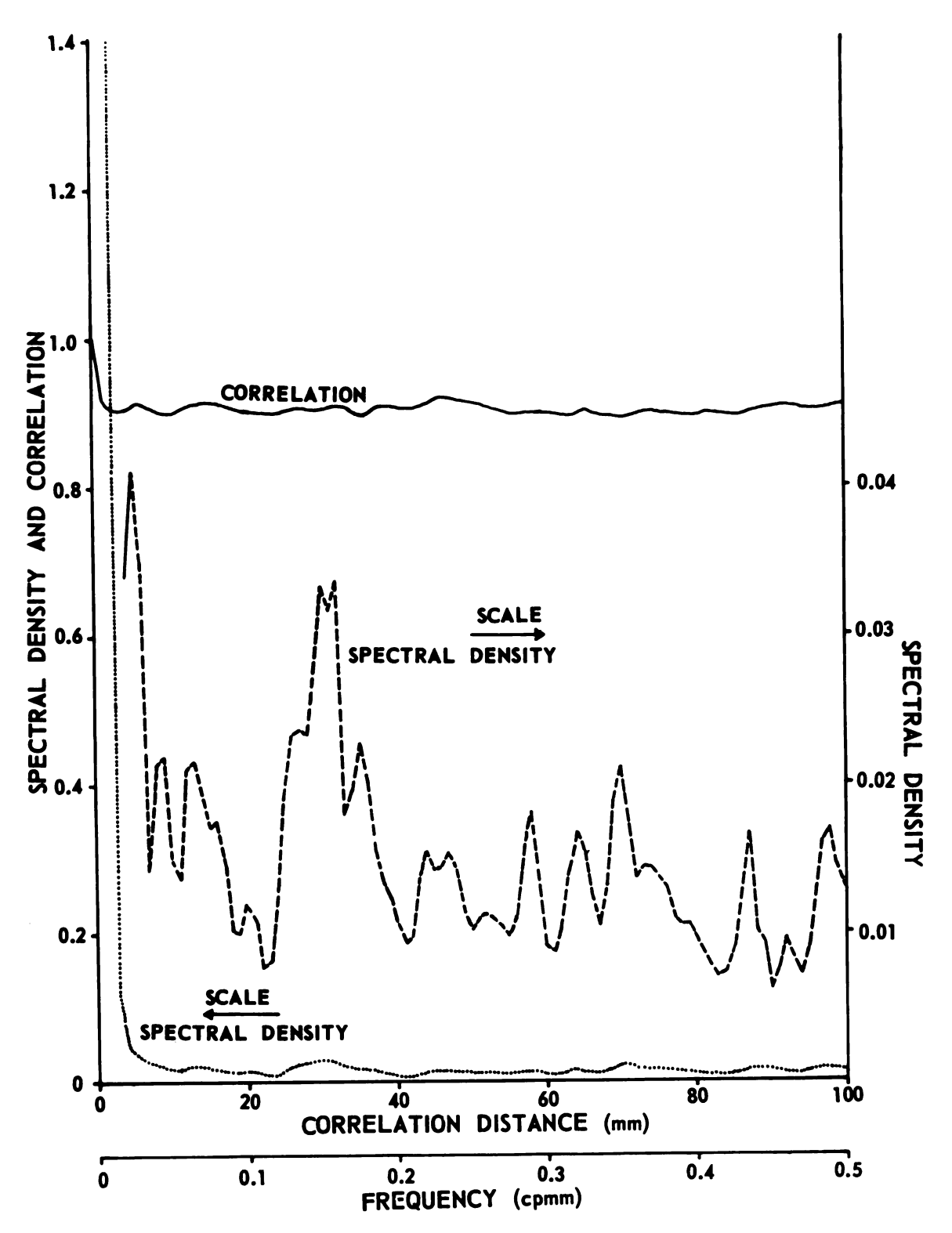


Figure 11. Spectral density and correlation of slopes of alfalfa stem relaxation curves

The portion of the spectral density curve from 0.075 cpmm is shown with 40X magnification (scale on right side of graph) to emphasize the fluctuations. Major peaks occur at 0.15 and 0.35 cpmm, but are probably not due to periodicities in the stem. Once again, more data are needed to determine the cause of these fluctuations.

Further research in the microstructures is needed to determine more exactly the physical structure of the alfalfa stem. Cell dimensions and orientation may give us a better idea as to the causes of certain fluctuations of the properties of the alfalfa stem.

VII. CONCLUSIONS

- 1. The location of the stem section selected to represent the relaxation characteristics of the alfalfa stem was not critical.
- 2. An equation of the form

logestress = A + Bloge time,

where A is the ordinate intercept and B is the slope of the curve, described the relaxation data of the alfalfa stem.

- 3. The cross-sectional area should be measured at, or within 0.75 millimeter of the point where the stress is applied to alfalfa stems.
- 4. It was necessary to account for alfalfa stem hollowness in determining applied stresses.
- 5. Considerable variation resulted in the measured cross-sectional area when an alfalfa stem configuration was assumed or when a microscope micrometer scale was used to measure the cross-sectional stem area.
- 6. The Flying-Spot Particle Analyser gave consistent results in crosssectional stem area measurement and measured the actual portion of the stem which contributes to the strength of the stem.

•

APPENDIX

RECOMMENDATIONS FOR FUTURE STUDY

- 1. Pool the data from more stems to resolve the lower frequencies of the spectral density analysis for cross-sectional areas and relaxation characteristics.
- 2. Investigate the microstructure of the alfalfa stem at various locations to determine the cause of fluctuations at certain frequencies in the spectral density analysis.
- 3. Compare field-grown alfalfa with greenhouse-grown alfalfa.

REFERENCES

- Bahn, A. K. (1959). Some Engineering Investigations of the Effects of Exposed Area on the Drying of Alfalfa. Thesis for the degree of M.S., Rutgers. New Brunswick, New Jersey. (Unpublished).
- Beran, M. (1965). Statistical Continuum Mechanics. Transactions of the Society of Rheology, 9:1, 339-355.
- Blackman, R. B., and J. W. Tukey. (1958). The Measurement of Power Spectra. Dover Publications, Inc., New York. 190 pp.
- Brazee, R. D., and F. Irons. (1965). The Flying-Spot Particle Analyzer. C.A. 53. Agricultural Engineering Research Division, Agricultural Research Service, United States Department of Agriculture. 11 pp.
- Ferry, J. D. (1961). Viscoelastic Properties of Polymers. John Wiley Wiley and Sons, Inc., New York. 482 pp.
- Ferry, J. D., and M. L. Williams. (1952). Second Approximation Methods for Determining the Relaxation Spectrum of a Viscoelastic Material. Journal of Colloid Science 7:347-353.
- Fitts, D. D. (1962). Nonequillibrium Thermodynamics. McGraw-Hill Book Company, Inc., New York. 173 pp.
- Halyk, R. M. (1962). Tensile and Shear Strength Characteristics of Alfalfa Stems. Thesis for the degree of M.S., University of Nebraska, Lincoln, Nebraska. (Unpublished).
- Handbook of Mathematical Functions, Apolied Mathematics Series 55, (1964). U. S. Department of Commerce, National Bureau of Standards, Washington, D.D. 1046 pp.
- Haywood, H. E. (1938). The Structure of Economic Plants. The Macmillan Company, New York. 674 pp.
- Instruction and Maintenance Manual (1964). Flying-Spot Particle Analyzer, Type 491. Airborne Instruments Laboratory, Division of Cutler-Hamner, Inc., Deer Park, Long Island, New York.
- Mansberg, H. P. (1964). Photo-Optical Field Measurement by Flying-Spot Scanners for Biomedical Applications. Society of Photographic Instrumentation Engineers Journal, Volume 2, February-March, 83-88.
- Martin, J. H., and W. H. Leonard. (1949). Principles of Field Crop Production. Macmillan Company, New York. 750 pp.

Manell, R., and J. Turney (1965). An Approach to Time Series Analysis.

Management Research Department, H. P. Hood and Sons, Boston, Massachusetts.

22 pp.

Papoulis, A. (1965). Probability, Random Variables and Stochastic Processes. McGraw-Hill Book Company, Inc., New York. 583 pp.

Prince, R. P., D. D. Wolf, and J. W. Bartok, Jr. (1965). The Physical Property Measurements of Forage Stalks. Bulletin 388, Agricultural Experiment Station, University of Connecticut, Storrs, Connecticut. 27 pp.

Wiener, N. (1956). Proceedings of the Third Berkeley Symposium on Mathematical Statistics and Probability, Volume III. University of California Press, Los Angeles, California. 252 pp.

Wilson, C. L., and W. E. Loomis. (1962). Botany. Holt, Rinehart and Winston, Inc.

Wilson, O. T. (1913). Studies on the Anatomy of Alfalfa. Kansas State Science Bulletin, Volume VII, Kansas State University, Lawrence, Kansas. 10 pp.

INDEX

A

ambient 23 antisymmetric 7 appendix 47 autocorrelation 17,18,19, 39,40

В

background 1
Beran 16
Bhan 23
biological 15,41
Blackmen 17,39

C

cambium 3 cathode-ray 24 collapse 31,32 collenchyma 3 comparison 22,34 component 7,8,9,15 computer 24 conclusions 46 condenser lens 24 continuous 9,11 correlation 15,16,18,19,20,39 40,41,43 counter 24 creep 2 cross-sectional 1,21,23,24,29 **34,35,38,39,46,**48 curve reader 32 cut-off saw 29

D

deflection 31 design 1 dismeter 23,29,34 (D cont.)

dimensional 2,3 discussion 34 distribution function 16 divergenceless 8 dyadic 7,8,9 dynamic 2

E

epidermis 3 expectation 17, 18 experiments 2 exponential 11

F

G

gamma function 12 growth 41

Η

Helyk 23 Heyward 2,3 hetergeneous 16 hollow 3,23,34,38 (H cont.)

hollowness 46 homogeneous 15

Ι

IBM 1620 32,39,41 impact 2 intensity 11 intercepts 24 intermodal 21,22,34 inversion 19,40

K

Kodak 24

L

lag 39, 40
Leonard 2
lignified 3
linear 9
load 31,32,39
load cell 31,32
logic 24
Loomis 3

M

Martin 2
mathematical 6,11,16,41
mean 15, 43
medium 7,8,9,15
Mennell 39
micrometer 23,29,31,34,35,46
microscope 3,29,31,34,35,38,46
model 11,16
moisture content 23
moments 16,19
monotonically 11
multiplier 24

N

negatives 24 node 21,22,29,31,34 normalized 39,43

0

oscillator 24 oscillograph 31

P

Papoulis 17
parenchymatous 3
Parzen 40
periodicities 15, 43
pith 3
photomicrograph 3
phototube 24
polygon 23
polymer 6,11
position 1,14,15,16
power spectrum 40
preamplifier 24
Prince 23
properties 1,6,15,16,23,39

R

random 15,16
raster 24
recorder 32
references 49
relative humidity 23
relaxation 1,2,7,8,11,12,21,
29,31,32,39,41,43,46,48
results 34
rheological 2
rigidity 11
rotation 8
round 23

S

X

xylem 3

sinusoidal 2 slope 14,18,32,41,43,46 spectral density 19,39,40,41, 43,45,48 spectrum 11 spectrum analysis 29,40 standard deviation 43 stem 1,2,3,6,21,22,23,24,29, 31, 32, 34, 38, 40, 41, 43, 45, 46,48 stoma 3 strain 2,7,8,9,10,12,13,14,15,16 stress 3,7,8,9,11,12,13,14,15,16, 17,23,31,46 structure 6 symmetric 7,8,10

T

temperature 9 tensor 7,8,9,16,20 threshold 24 tracheal 3 transient 2 translation 9 transmission 24,29 trends 15,40,43 truncation 40 Tukey 17,39 Turney 39 twisting 31

V

veriation 1,46 vector 7,8 viscoelastic 2,6,7,8,15,16 viscoplastic 2

W

Wilson 3 Williams 12,13



